Quantifying the elastic deformation behavior of bridged nanobelts

Wenjie Mai and Zhong Lin Wang[a)]
School of Materials Science and Engineering, Georgia Institute of Technology, Atlanta, Georgia 30332-0245

(Received 5 June 2006; accepted 27 June 2006; published online 17 August 2006)

A new approach for quantifying the elastic deformation behavior of one-dimensional nanostructures is presented by fitting the image profile measured using atomic force microscopy in contact mode along the entire length of a bridged/suspended nanobelt/nanowire/nanotube under different load forces. Consistently fitting the measured deformation profiles can uniquely determine if the measured data are best explained by either the clamped-clamped beam model or the free-free beam model without preassumption, and it eliminates the uncertainty in defining the central point of the suspended beam, thus, greatly increasing the precision and reliability of the measurements. © *2006 American Institute of Physics*. [DOI: 10.1063/1.2336600]

One-dimensional (1D) nanomaterials, such as carbon nanotubes,[1–3] semiconductor nanowires,[4] and oxide nanobelts,[5] are the fundamental building blocks for constructing nanodevices and nanosystems that exhibit superior performances. Mechanical behavior of 1D nanomaterials is one of the most important properties that dictate their applications in nanotechnology. Various methods have been developed for quantifying the mechanical property of 1D nanomaterials, and they may be classified into three categories. The first approach is based on dynamic resonance of a 1D nanostructure that is affixed at one end and free at the other; the mechanical resonance is excited by an externally applied oscillating electrical field, and the observation is made through electron microscopy.[6,7] The second approach is quantifying the static axial tensile stretching of a 1D nanostructure using an atomic force microscope (AFM) tip, which is installed inside a scanning electron microscope (SEM).[2] The third approach is based on AFM and nanoindenter.[8–13] One of the most important and common strategies is deforming a 1D nanostructure that is supported at the two ends using an AFM tip, which pushes the 1D nanostructure at its middle point. Quantifying the middle-point force-displacement curve gives the elastic modulus. The accuracy of this measurement is, however, limited by the size of the tip and the accuracy of positioning the AFM tip right at the middle of the 1D nanostructure due to the unavoidable hysteresis of the piezoceramic actuator of the AFM cantilever.

In this letter, we present a new approach for quantifying the elastic deformation behavior of a 1D nanostructure. Our approach is based on a continuous scan of a ZnO nanobelt (NB) that is supported at the two ends by an AFM tip in contact mode; a quantitative fitting of the elastic bending shape of the NB as a function of the bending force provides a reliable and accurate method for measuring the elastic modulus of the NB.

The ZnO NBs used for this study were prepared by physical vapor deposition.[5] A silicon substrate is prepared with long and parallel trenches caved at its surface by nanofabrication. The trenches are about 200 nm deep and 1.25 μm wide [Fig. 1(a)]. Long ZnO NBs were manipulated across the trenches over many periods. The morphology and dimensions of the NB were captured by SEM and AFM. The SEM image gives the width of the trench and the length and width of the NB, and the AFM image gives the thickness of the NB [Figs. 1(b) and 1(c)]. The measurement was made by scanning the NB along its length direction using an AFM tip in contact mode at a constant applied force. A series of bending images of the NB were recorded by changing the magnitude of the contact force, from which the elastic deformation behavior of the NB is derived based on model calculation. The AC240 cantilevers (spring constant of ~2 N/m) from Asylum Research were used in our research, and each cantilever was carefully calibrated using the method of Sader *et al.*,[14] so that the AFM contact forces could be calculated.

The profiles of a suspend NB along the length direction under different contact forces are showed in Fig. 2(a). Each curve was received by an average of ten consecutive measurements along its length under the same loading force. Due to a small surface roughness (~1 nm) of the NB, the curves are not perfectly smooth. In addition, the as-attached NB on the trenches is not perfectly straight, possibly due to initial bending during the sample manipulation. In order to eliminate the effect of the surface roughness and initial bending of

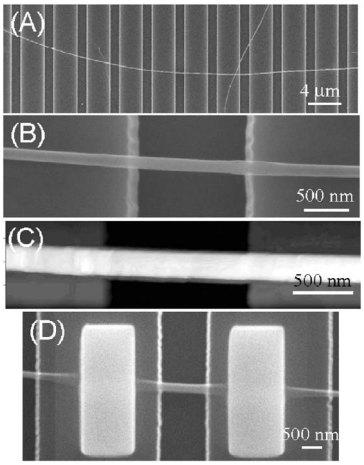

FIG. 1. (a) Low-magnification SEM image of a silicon substrate with parallel trenches. Long nanobelts (NBs) are lying on the trenches. (b) SEM image of one NB bridged over a trench (c) and the corresponding AFM image of the bridged NB over the trench. (d) The corresponding SEM image of the same NB in (b) after depositing Pt pads at the two ends.

[a)]Author to whom correspondence should be addressed; electronic mail: zhong.wang@mse.gatech.edu

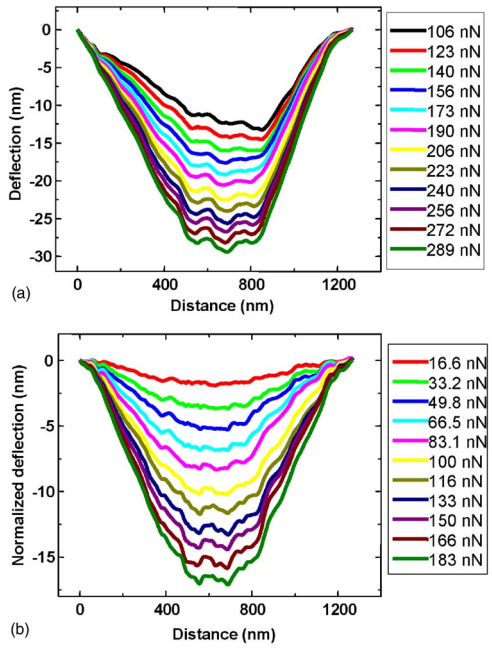

FIG. 2. (Color online) (a) As-received AFM image profiles of one suspended NB under different load forces in contact mode. (b) The normalized AFM image profile after removing the surface roughness by subtracting the image acquired at 106 nN from the data in (a). The force is also normalized in reference to the "zero setting point" of 106 nN.

the NB on force curve quantification, deflection curves are calibrated by subtracting the profile measured under low applied force (~100 nN) from those measured at higher applied forces. Due to the presence of the trench, a reasonable force has to be applied to make the tip in contact with the NB. To obtain a good image under common AFM, the set point was chosen to be ~0.5 V, which corresponded to ~100 nN for the AFM we used. As a result a normalized force is also defined by subtracting the 100 nN from the applied force, and the final results are shown in Fig. 2(b). Some small ripples appear at the middle of the NB and become pronounced with the increase in contact force. This may be due to the rippling effect of the NB with a compressed top surface in contacting with the AFM tip, because the ZnO NB cannot easily create and preserve edge dislocations to accommodate the deformation.

For all of the measurements, the load was kept small so that the maximum deflection of the NB is less than the half thickness of the NB. It is very reasonable to assume that the deformation process is elastic. The AFM scanning rate was kept at 0.5~1 Hz; thus, the measurement is static. The measurements were repeated by increasing and decreasing the load to ensure the reproducibility in the profile (within 1 nm) and negligible hysteresis. This is important for the data analysis using elastic deformation theory.

The profile images of the NB recorded the deformation of all of the points along its length under different applied forces. One profile could contain up to 650 points. Every point on the suspended portion of NB in the images can be regarded as a mechanical measurement done using the approaches in the literature.[15,16] By fitting the shapes of all of the curves measured at different applied forces, the elastic modulus can be derived reliably and precisely. The question now is what model will be used to quantify the data.

There are two typical models derived under different boundary conditions. One is the clamped-clamped beam model (CCBM) [Fig. 3(a)], in which the two ends of the NB are affixed, so that the deflection v and its first derivative dv/dx are both 0 at $x=0$ and $x=L$, where L is the width of the trench. The other is the free-free beam model (FFBM) [Fig. 3(b)], in which the two ends of the NB can freely slide, which means that only the support force exists and there is no force moment; thus, only $v=0$ at $x=0$ and $x=L$. When a concentrated load F is applied at point a away from the A end, the differential equation that determines the deflection of the entire beam under small angle deformation is

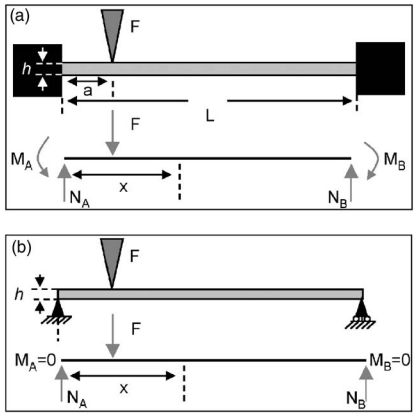

FIG. 3. Schematic diagrams of the (a) clamped-clamped beam model (CCBM) and (b) the free-free beam model (FFBM).

$$EI\frac{d^2v}{dx^2} = -N_A x + F[x-a] + M_A, \tag{1}$$

where E is the bending modulus, I the moment of inertia given by $wh^3/12$ for the rectangular beam, N_A the support force and M_A the force moment at the A end, and $[x-a]$ is a step function, which means that $[x-a]=1$ when $x \geqslant a$ and $[x-a]=0$ when $x<a$. In the CCBM, the solution of Eq. (1) is

$$v = \frac{Fa^3(L-a)^3}{3EIL^3}. \tag{2}$$

This equation gives the deflection of the NB at the contact point a of the AFM tip under a constant applied force F. In the FFBM, the deflection of the NB at the contact point a is

$$v = \frac{Fa^2(L-a)^2}{3EIL}. \tag{3}$$

Also, it is also possible to have clamped-free mixed case, and v will have an asymmetric form. But such a case was not detected in our experiment.

In the literature,[11,13] the CCBM theory was assumed because it was assumed that the adhesion force between the 1D nanostructure and the substrate was strong enough to clamp the two ends of the nanostructure. The argument was that the nanostructure could bear a relatively large lateral force without any observable movement. Some researchers begin to deposit some metal pads to satisfy the CCBM conditions.[12] From the discussion given above, the two different models give totally different results. For instance, at the middle point $a=L/2$, $E=FL^3/192Iv$ for CCBM, and $E=FL^3/48Iv$ for the FFBM, which are different by a factor of 4 in the measured elastic modulus. But one is unable to truly identify the

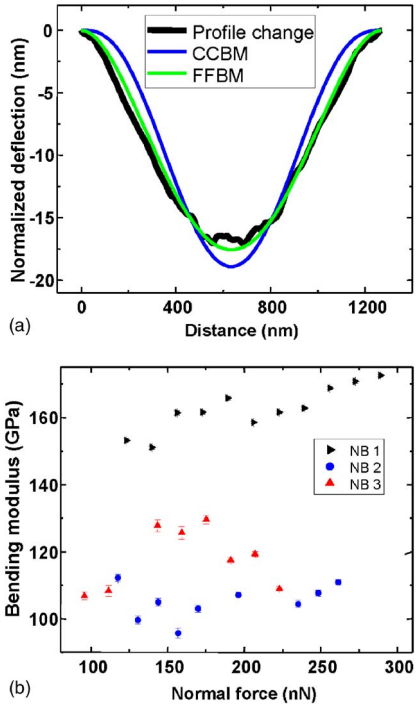

FIG. 4. (Color online) (a) Curve fitting using the CCBM and FFBM for the image profiles of NB 1 acquired under normalized force of 183 nN. (b) The bending modulus from the FFBM fitted curves under different load forces. The error bars are introduced with consideration of the uncertainty in curve fitting. The dimensions of NB 1 are 1.270 μm in length, 90 nm in width, and 70 nm in thickness; the dimensions of NB 2 are 1.253 μm in length, 115 nm in width, and 95 nm in thickness; and the dimensions of NB 3 are 1.232 μm in length, 125 nm in width, and 115 nm in thickness.

model for data analysis if the measurement is made only at one contact point, such as the middle point, of the 1D nanostructure.

From Eqs. (2) and (3), it is apparent that the shapes of two deformation curves for the two models are different and the slopes of the curves are dramatically different. Therefore, by fitting the shape of the curve measured experimentally under different applied forces, it will be unique to determine which model is more precise to quantify the elastic deformation behavior of the NB. This is our principle for data analysis. Figure 4(a) shows an example of curve fitting based on the two models. The FFBM is found to fit much better than the CCBM, especially when the applied force is large ($>$190 nN). Under lower applied force, the surface roughness of the NB and the noise from the AFM system make it more difficult to judge the best fit.

To examine the validity of the FFBM for modeling the results presented in Fig. 4(a), elastic deformation was made from a NB before and after affixing the two ends. Figure 1(d) shows a SEM image of a NB after depositing two Pt pads at the two ends by focus ion beam microscopy. Before Pt deposition, the maximum relative deflection of the NB at the middle point was measured to be 5.4 nm at a normalized force of 117 nN. After Pt deposition, the maximum relative deflection of the NB decreased to 1–1.5 nm at a normalized force of 119 nN. The ratio is $\sim$4, in agreement with the expected result from the theory. This test indicates that the elastic deformation behavior of a bridged NB with two ends "free" can be reliably modeled using FFBM.

From a general understanding that, at a large load force, the friction between the NB and the edge of the trench may be large enough to prevent the sliding of the NB, then the result could be approximately modeled by the CCBM although the two ends are unfixed. In contrast, we found that the adhesion between the ZnO NB and the silicon substrate is weak, possibly due to the incompatible crystal structure systems and the large lattice mismatch. ZnO NBs can often be displaced by AFM tip during imaging, although the scanning direction is along the NB for minimizing the possibility of large impact from the AFM tip. In our case, the adhesion force and the force moment at each side of the NB can be regarded as zero, so that the FFBM is the most reasonable model.

Figure 4(b) shows the bending modulus derived from the curve fitting at different loads for three different NBs. The elastic moduli for NBs 1, 2, and 3 remain consistent, respectively, under different loaded forces, indicating that the deformation is elastic although ripples have been observed from the deformation curve [Fig. 2(b)]. The elastic moduli for NBs 1, 2, and 3 are 162 ± 12, 105 ± 10, 118 ± 14 GPa, respectively. The difference for the three NBs is likely related to their sizes. The bending modulus presented here is larger than that measured by mechanical resonance measured by *in situ* TEM.[17]

The authors thank Jin Liu, Changshi Lao, and Tsuyoshi Yamashita for many discussions and help and NSF, the NASA Vehicle Systems Program and Department of Defense Research and Engineering (DDRE), and the Defense Advanced Research Projects Agency for support.

[1] T. W. Odom, J. L. Huang, P. Kim, and C. M. Lieber, Nature (London) **391**, 62 (1998).
[2] M. F. Yu, O. Lourie, M. J. Dyer, K. Moloni, T. F. Kelly, and R. S. Ruoff, Science **287**, 637 (2000).
[3] S. Frank, P. Poncharal, Z. L. Wang, and W. A. de Heer, Science **280**, 1744 (1998).
[4] Y. Cui and C. M. Lieber, Science **291**, 851 (2001).
[5] Z. W. Pan, Z. R. Dai, and Z. L. Wang, Science **291**, 1947 (2001).
[6] P. Poncharal, Z. L. Wang, D. Ugarte, and W. A. de Heer, Science **283**, 1513 (1999).
[7] A. P. Suryavanshi, M. F. Yu, J. G. Wen, C. C. Tang, and Y. Bando, Appl. Phys. Lett. **84**, 2527 (2004).
[8] E. W. Wong, P. E. Sheehan, and C. M. Lieber, Science **277**, 1971 (1997).
[9] J. H. Song, X. D. Wang, E. Riedo, and Z. L. Wang, Nano Lett. **5**, 1954 (2005).
[10] X. D. Li, X. N. Wang, Q. H. Xiong, and P. C. Eklund, Nano Lett. **5**, 1982 (2005).
[11] J. P. Salvetat, G. A. D. Briggs, J. M. Bonard, R. R. Bacsa, A. J. Kulik, T. Stockli, N. A. Burnham, and L. Forro, Phys. Rev. Lett. **82**, 944 (1999).
[12] B. Wu, A. Heidelberg, and J. J. Boland, Nat. Mater. **4**, 525 (2005).
[13] G. Y. Jing, H. Ji, W. Y. Yang, J. Xu, and D. P. Yu, Appl. Phys. A: Mater. Sci. Process. **82**, 475 (2006).
[14] J. E. Sader, J. W. M. Chon, and P. Mulvaney, Rev. Sci. Instrum. **70**, 3967 (1999).
[15] J. M. Gere, *Mechanics of Materials* (Brooks-Cole, Boston, 2001), Vol. 8, p. 445.
[16] P. P. Benham, R. J. Crawford, and C. G. Armstrong, *Mechanics of Engineering Materials* (Essex, England, 1996), Vol. 8, p. 213.
[17] X. D. Bai, P. X. Gao, Z. L. Wang, and E. G. Wang, Appl. Phys. Lett. **82**, 4806 (2003).